



# Mutating a conserved cysteine in GPIHBP1 reduces amounts of GPIHBP1 in capillaries and abolishes LPL binding<sup>S</sup>

Christopher M. Allan,\* Cris J. Jung,<sup>†</sup> Mikael Larsson,\* Patrick J. Heizer,\* Yiping Tu,\* Norma P. Sandoval,\* Tiffany Ly P. Dang,\* Rachel S. Jung,\* Anne P. Beigneux,<sup>1,\*</sup> Pieter J. de Jong,<sup>†</sup> Loren G. Fong,<sup>1,\*</sup> and Stephen G. Young<sup>1,\*§</sup>

Departments of Medicine\* and Human Genetics,<sup>§</sup> David Geffen School of Medicine, University of California Los Angeles, Los Angeles, CA 90095; and Children's Hospital Oakland Research Institute,<sup>†</sup> Oakland, CA 94609

**Abstract** Mutation of conserved cysteines in proteins of the Ly6 family cause human disease—chylomicronemia in the case of glycosylphosphatidylinositol-anchored HDL binding protein 1 (GPIHBP1) and paroxysmal nocturnal hemoglobinuria in the case of CD59. A mutation in a conserved cysteine in CD59 prevented the protein from reaching the surface of blood cells. In contrast, mutation of conserved cysteines in human GPIHBP1 had little effect on GPIHBP1 trafficking to the surface of cultured CHO cells. The latter findings were somewhat surprising and raised questions about whether CHO cell studies accurately model the fate of mutant GPIHBP1 proteins in vivo. To explore this concern, we created mice harboring a GPIHBP1 cysteine mutation (p.C63Y). The p.C63Y mutation abolished the ability of mouse GPIHBP1 to bind LPL, resulting in severe chylomicronemia. The mutant GPIHBP1 was detectable by immunohistochemistry on the surface of endothelial cells, but the level of expression was ~70% lower than in WT mice. The mutant GPIHBP1 protein in mouse tissues was predominantly monomeric. We conclude that mutation of a conserved cysteine in GPIHBP1 abolishes the ability of GPIHBP1 to bind LPL, resulting in mislocalization of LPL and severe chylomicronemia. The mutation reduced but did not eliminate GPIHBP1 on the surface of endothelial cells in vivo.—Allan, C. M., C. J. Jung, M. Larsson, P. J. Heizer, Y. Tu, N. P. Sandoval, T. L. P. Dang, R. S. Jung, A. P. Beigneux, P. J. de Jong, L. G. Fong, and S. G. Young. **Mutating a conserved cysteine in GPIHBP1 reduces amounts of GPIHBP1 in capillaries and abolishes LPL binding.** *J. Lipid Res.* 2017. 58: 1453–1461.

**Supplementary key words** chylomicrons • endothelial cells • lipids/chemistry • lipolysis and fatty acid metabolism • triglycerides • glycosylphosphatidylinositol-anchored HDL binding protein 1 • lipoprotein lipase

This work was supported by National Heart, Lung, and Blood Institute Grants HL090553, HL087228, and HL125335 and a Transatlantic Network grant from Fondation Leducq (12CVD04). Additional support was provided by a Ruth L. Kirschstein National Research Service Award, National Institutes of Health Grant T32HL69766 to C.M.A. The content is solely the responsibility of the authors and does not necessarily represent the official views of the National Institutes of Health. The authors have no financial interests to declare.

Manuscript received 12 April 2017 and in revised form 4 May 2017.

Published, JLR Papers in Press, May 5, 2017  
DOI <https://doi.org/10.1194/jlr.M076943>

Glycosylphosphatidylinositol-anchored HDL binding protein 1 (GPIHBP1), a GPI-anchored protein of capillary endothelial cells, binds LPL in the interstitial spaces (where it is secreted by myocytes and adipocytes) and transports it across endothelial cells to the capillary lumen (1). When GPIHBP1 production is absent, LPL never reaches the capillary lumen, resulting in defective intravascular triglyceride processing and severe hypertriglyceridemia (chylomicronemia) (1, 2). GPIHBP1 is a member of the Ly6 family of proteins and contains two principal domains—an N-terminal acidic domain followed by a three-fingered Ly6 domain containing 10 cysteines (3). The 10 cysteines form five disulfide bonds that maintain the three-fingered structure of the Ly6 domain (4). An early report suggested that the acidic domain played an important role in LPL binding (5), but recent studies with more refined LPL–GPIHBP1 binding assays showed that the Ly6 domain is primarily responsible for LPL binding, with the acidic domain playing a smaller, accessory role (3).

Since the discovery of GPIHBP1's role in intravascular triglyceride processing (2), many *GPIHBP1* mutations have been identified in patients with familial chylomicronemia (6–11). In some cases, deletions of the entire gene have been documented (12, 13), but most of the mutations have been missense mutations that interfere with GPIHBP1's ability to bind LPL (6–11, 14). Many missense mutations involve one of the conserved cysteines in the Ly6 domain or an adjacent residue (6, 7, 9, 10). In CHO cell studies, these mutations promote the formation of

Abbreviations: BAT, brown adipose tissue; ER, endoplasmic reticulum; GPIHBP1, glycosylphosphatidylinositol-anchored HDL binding protein 1; LDLR, LDL receptor; mAb, monoclonal antibody; PIPLC, phosphatidylinositol-specific phospholipase C; WAT, white adipose tissue.

<sup>†</sup>To whom correspondence should be addressed.

e-mail: lfong@mednet.ucla.edu (L.G.F.); abeigneux@mednet.ucla.edu (A.P.B.); sgyoung@mednet.ucla.edu (S.G.Y.)

<sup>S</sup>The online version of this article (available at <http://www.jlr.org>) contains a supplement.

inappropriate intermolecular disulfide bonds, leading to protein dimerization/multimerization (11, 15). GPIHBP1 dimers and multimers have no ability to bind LPL. Thus far, no one has identified a clinically significant mutation in GPIHBP1's acidic domain.

In studies with transfected CHO cells, mutation of any one of the 10 cysteines in the Ly6 domain in human GPIHBP1 abolished the ability of GPIHBP1 to bind LPL (16); however, these mutations have little or no effect on the amount of GPIHBP1 that reaches the cell surface (15–17). In contrast, a *GPIHBP1* missense mutation that abolished N-linked glycosylation markedly reduced GPIHBP1 trafficking to the cell surface (17, 18). The fact that Ly6 domain cysteine mutants behaved differently than the glycosylation mutant was surprising—for several reasons. First, cysteine mutations in cysteine-rich repeats within the epidermal growth factor precursor homology domain of the LDL receptor (LDLR) cause protein misfolding, preventing the LDLR from moving from the endoplasmic reticulum (ER) to the Golgi (19). Second, mutation of a cysteine in the Ly6 domain of CD59 abolished CD59 trafficking to the surface of blood cells (resulting in increased complement activation and paroxysmal nocturnal hemoglobinuria) (20). In light of the latter observations, we were concerned that the finding of normal trafficking of GPIHBP1 cysteine mutants to the surface of CHO cells may have represented an artifact of protein overexpression (i.e., that overexpression of GPIHBP1 mutants overwhelmed the ER quality-control surveillance mechanisms that would ordinarily remove misfolded proteins).

In the current studies, we sought to determine whether a mutation in a conserved cysteine in GPIHBP1's Ly6 domain would prevent GPIHBP1 from reaching the surface of endothelial cells in vivo. To address this issue, we generated mutant mice harboring a p.C63Y mutation in *Gpihbp1* [a mutation first identified in a 3-year-old boy with chylomicronemia (9)]. Cys-63, the first of 10 cysteines in the Ly6 domain, is disulfide bonded to the fifth cysteine (Cys-88), creating the first finger of GPIHBP1's Ly6 domain (17).

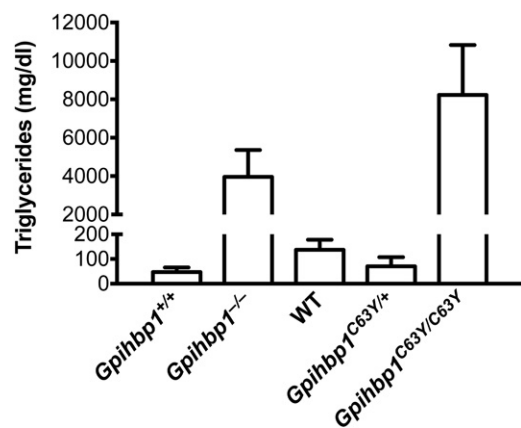


**Fig. 1.** Severe hypertriglyceridemia in *Gpihbp1*<sup>-/-</sup> and *Gpihbp1*<sup>C63Y/C63Y</sup> mice. Plasma triglyceride levels were measured in plasma samples from 3.5- to 4-month-old *Gpihbp1*<sup>-/-</sup> and littermate WT mice (*Gpihbp1*<sup>+/+</sup>) (n = 5/group) along with *Gpihbp1*<sup>C63Y/C63Y</sup> mice and littermate *Gpihbp1*<sup>C63Y/+</sup> and WT mice (n = 6/group).

A second objective was to test the primacy of GPIHBP1's Ly6 domain in LPL binding. We sought to determine whether an Ly6 domain point mutation—which leaves the acidic domain intact—would permit residual LPL binding and therefore be associated with milder disease than in *Gpihbp1*<sup>-/-</sup> mice (1, 2, 21), where all of the protein-coding sequences were deleted.

## MATERIALS AND METHODS

### Generation of *Gpihbp1*<sup>C63Y/C63Y</sup> mice

Zygotes from FVB females were injected with 10 ng Cas9n mRNA transcript, 5 ng sgRNA transcript, and 20 ng single-stranded oligonucleotides at the Transgenic Core Facility of the Gladstone Institutes (San Francisco, CA). To generate a mutant allele containing the p.C63Y, oligonucleotides were obtained from IDTDNA as ultramers of 150 nucleotides (5'-TTAGGCATGGCCTTGGAGTCTCTCTCTCTCAATCTGAGCTGCCCTGCCA-CACACAGCACCTCTACAATATTACTTCTGTCAAGTGCTTCA-CAGCGGGGAGAGCTGCAATCAGACACAGAGCTGCTCCAGC-AGCAAACCCCTTCTGCATCAC-3'; mutation in bold; *SspI* restriction site underlined). We used either Cas9 or Cas9n mRNA transcripts for oligonucleotide targeting. Cas9 was coinjected with a single sgRNA (5'-TGACAGAAGTAGCATTGTAGAGG-3'), whereas Cas9n was coinjected with two sgRNAs (5'-GTAGCATTGTAGAGGTGCTGTGG-3'; 5'-CTGTCAAGTGCTTACAGCGGGG-3') designed to create nicks on opposite strands of DNA, creating a 5' overhang. sgRNA transcripts were created with MEGAscript T7 kit (ThermoFisher Scientific) and purified with the MEGAclear kit (ThermoFisher Scientific). Cas9 and Cas9n mRNA transcripts were purchased from TriLink. All transcripts were frozen at -80°C prior to the microinjection procedure. Genotyping of mice was performed by standard PCR with oligonucleotides

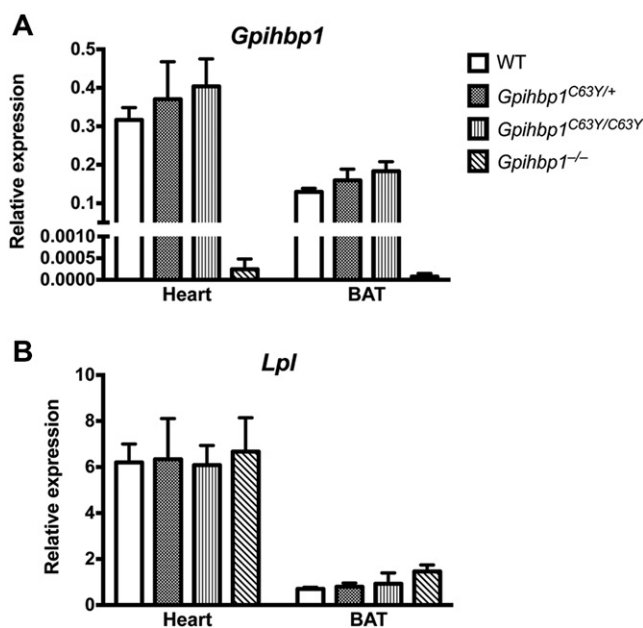


**Fig. 2.** *Gpihbp1* and *Lpl* transcript levels in heart and BAT from 2-month-old *Gpihbp1*<sup>C63Y/C63Y</sup>, *Gpihbp1*<sup>C63Y/+</sup>, and WT mice along with *Gpihbp1*<sup>-/-</sup> mice. *Gpihbp1* (A) and *Lpl* (B) transcript levels were measured by qRT-PCR (n = 3 for WT, *Gpihbp1*<sup>C63Y/C63Y</sup>, and *Gpihbp1*<sup>-/-</sup> mice; n = 4 for *Gpihbp1*<sup>C63Y/+</sup> mice). Transcript levels were normalized to expression of cyclophilin A.

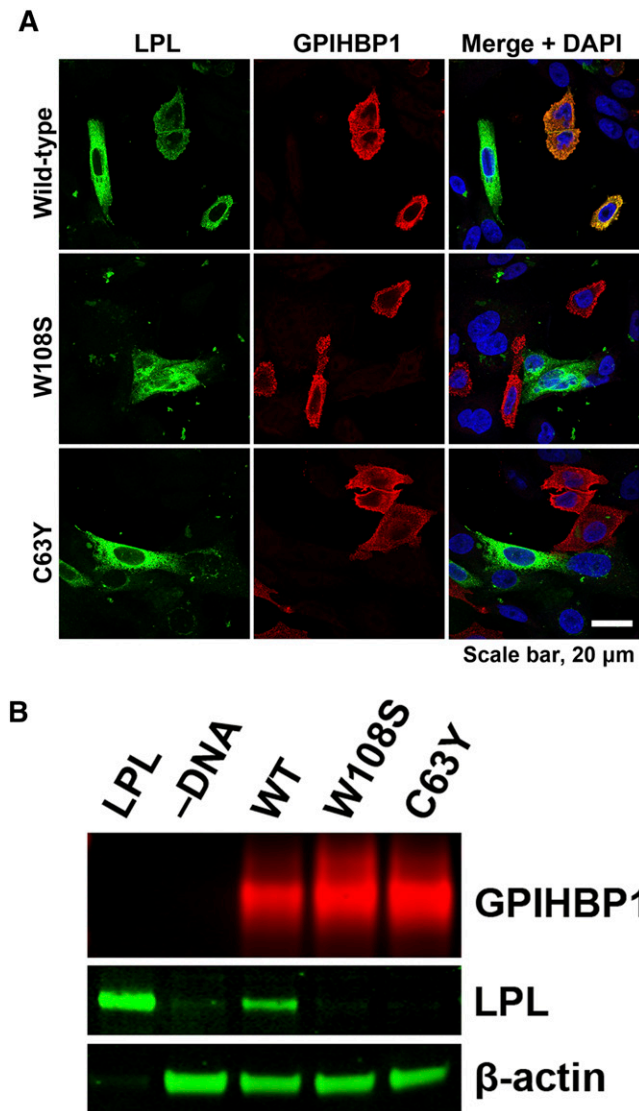


**Fig. 3.** GPIHBP1-C63Y cannot bind LPL. **A:** Testing binding of V5-tagged mouse LPL to WT GPIHBP1, GPIHBP1-W108S, and GPIHBP1-C63Y in a co-plating assay (17). In earlier studies, we showed that human GPIHBP1-W109S and human GPIHBP1-C65Y were unable to bind human LPL (9, 15). Here, CHO pgsA-745 cells were electroporated with either an S-protein-tagged version of GPIHBP1 or an expression vector for V5-tagged LPL. The independently transfected cells were then mixed together and plated on coverslips in 24-well plates. Twenty-four hours later, the cells were processed for immunocytochemistry with a goat antibody against the S-protein tag and a mAb against the V5 tag. DNA was stained with DAPI. In this system, cells that expressed WT GPIHBP1 captured LPL produced by LPL-transfected cells; hence, GPIHBP1 and LPL signals colocalized on the merged image. GPIHBP1-W108S and GPIHBP1-C63Y did not bind LPL; hence, there was no colocalization of LPL and GPIHBP1 on the merged image. **B:** Absent binding of V5-tagged LPL to mouse GPIHBP1-W108S and GPIHBP1-C63Y. CHO pgsA-745 cells were electroporated with S-protein-tagged versions of GPIHBP1 expression vectors. Twenty-four hours after the electroporation, cells were incubated with V5-tagged human LPL. After 1 h, cell extracts were prepared, and the amount of LPL bound to the cells was assessed by Western blotting with an antibody against the V5-tag. The amount of GPIHBP1 in cell extracts was assessed with an antibody against the S-protein tag. The first lane of the Western blot (“LPL”) shows the LPL preparation that was added to the GPIHBP1-transfected cells; the lane labeled (“-DNA”)

5'-GACCCGGAGCCAGAGAACTA-3' (forward) and 5'-TGGTC-CAGCCTGAAGGTAT-3' (reverse). The 1,000 bp product was digested at 37°C for 2 h with *Ssp*I-HF (New England Biolabs). Gel electrophoresis was used to resolve the products, with the WT allele yielding 783 and 217 bp bands, and the mutant allele yielding 462, 321, and 217 bp bands. The mice were fed a chow diet and housed in a barrier facility with a 12 h light-dark cycle. All studies were approved by the University of California Los Angeles' Animal Research Committee.

### Measuring plasma triglycerides

Blood was collected from 3.5- to 4-month-old mice by retro-orbital bleeding. Triglycerides were measured in plasma samples with the triglyceride determination kit (Sigma Aldrich) according to the manufacturer's instructions.

### Testing the ability of LPL to bind to GPIHBP1-C63Y by immunocytochemistry

The ability of several GPIHBP1 constructs to bind LPL was tested with a “co-plating assay” (17). CHO pgsA-745 cells ( $5 \times 10^5$ ) were electroporated with either 0.5  $\mu$ g of a plasmid for S-protein-tagged versions of mouse WT GPIHBP1, GPIHBP1-W108S, or GPIHBP1-C63Y. These cells were then mixed with CHO pgsA-745 cells ( $5 \times 10^5$ ) that had been independently electroporated with 0.5  $\mu$ g of a plasmid for V5-tagged mouse LPL and plated on coverslips in 24-well plates. After 24 h, cells were fixed with 3% paraformaldehyde for 15 min and processed for immunocytochemistry. Cells were permeabilized with 0.2% Triton X-100 and blocked with 10% donkey serum in PBS/Ca/Mg. Cells were then incubated overnight at 4°C with a mouse monoclonal antibody (mAb) against the V5 tag (ThermoFisher Scientific; 1:100) and a goat polyclonal antibody against the S-protein tag (Abcam; 1:800), followed by a 30 min incubation with an Alexa568-conjugated donkey anti-goat IgG (ThermoFisher Scientific; 1:800) and an Alexa488-conjugated donkey anti-mouse IgG (ThermoFisher Scientific; 1:800). After washing, the cells were fixed with 3% paraformaldehyde for 15 min and stained with DAPI to visualize DNA. Images were recorded with an Axiovert 200M microscope and processed with Zen 2010 software (all from Zeiss). Within each experiment, the exposure conditions for each construct were identical.

### Testing the ability of LPL to bind to GPIHBP1-C63Y by Western blotting

CHO pgsA-745 cells ( $2 \times 10^6$ ) were electroporated with 2  $\mu$ g S-protein-tagged versions of the WT or mutant GPIHBP1 vectors (GPIHBP1-W108S, GPIHBP1-C63Y). After 24 h, cells were incubated with V5-tagged human LPL for 1 h at 4°C (22). After washing cells twice with PBS, cell extracts were prepared using M-PER mammalian protein extraction reagent (ThermoFisher Scientific) with Complete EDTA-free protease inhibitor cocktail (Roche). Extracts were size-fractionated on 12% NuPAGE SDS-PAGE gels with MES buffer, followed by transfer to a nitrocellulose membrane. The membranes were blocked for 1 h at room temperature with Odyssey blocking buffer (LI-COR). The amount of LPL bound to the cells was assessed by Western blotting with an antibody against the V5 tag. The amount of GPIHBP1 in cell extracts was assessed with an antibody against the S-protein tag. Actin was used as a loading control.

indicates extracts of nontransfected cells; the lanes labeled WT, W108S, and C63Y show extracts of cells that had been transfected with expression vectors for WT mouse GPIHBP1, GPIHBP1-W108S, or GPIHBP1-C63Y, respectively. Actin was used as a loading control.

## Immunohistochemistry on mouse tissues

Mice were anesthetized with isoflurane and perfused with PBS followed by 3% paraformaldehyde. The brown adipose tissue (BAT), heart, and quadriceps were then harvested and embedded in OCT medium on dry ice. Tissue sections (7  $\mu\text{m}$  for heart and quadriceps; 10  $\mu\text{m}$  for BAT) were fixed with methanol at  $-20^{\circ}\text{C}$  for 10 min, permeabilized with 0.2% Triton X-100 for 5 min, and blocked at room temperature with 5% donkey serum and 0.2% BSA in PBS/Mg/Ca. Tissues were incubated overnight at  $4^{\circ}\text{C}$  with a goat polyclonal antibody against mouse LPL (12  $\mu\text{g}/\text{ml}$ ) (23) and a rabbit polyclonal antibody against mouse CD31 (Abcam; 1:50), followed by a 45 min incubation at room temperature

with Alexa647-conjugated antibody 11A12 (3  $\mu\text{g}/\text{ml}$ ), Alexa568-conjugated donkey anti-goat IgG (ThermoFisher Scientific; 1:200), and Alexa488-conjugated donkey anti-rabbit IgG (ThermoFisher Scientific; 1:200). After washing, the tissues were fixed with 3% paraformaldehyde for 5 min and stained with DAPI to visualize DNA. Images were recorded with an Axiovert 200M microscope and processed with Zen 2010 software (all from Zeiss). Within each experiment, the exposure conditions for each construct were identical.

## Quantifying *Lpl* and *Gpihbp1* transcripts

Mice were anesthetized with isoflurane and perfused with PBS. The BAT and heart were harvested and flash-frozen in

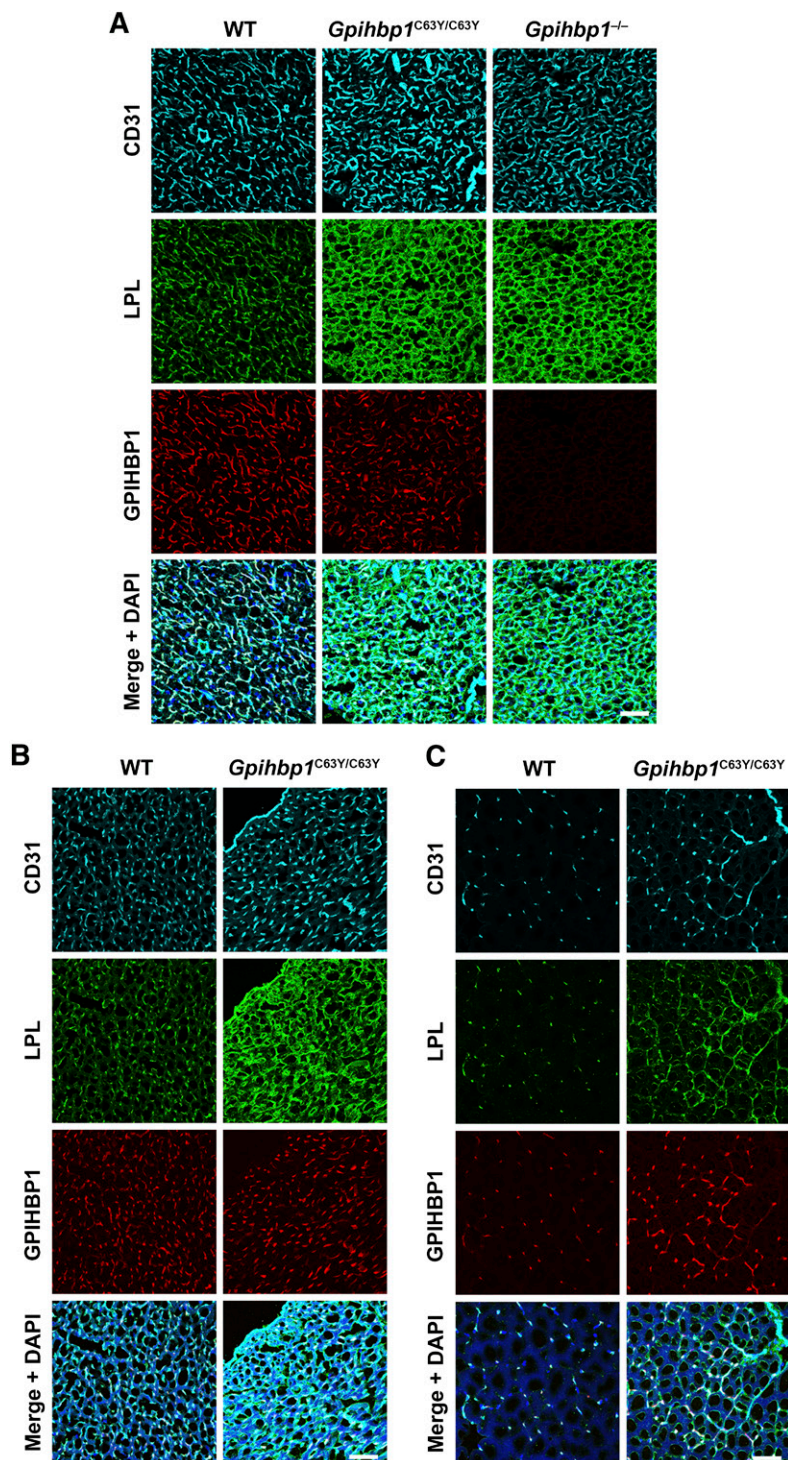


**Fig. 4.** LPL is mislocalized within the interstitial spaces in *Gpihbp1*<sup>C63Y/C63Y</sup> and *Gpihbp1*<sup>-/-</sup> mice. Immunohistochemistry studies were performed on sections of BAT (A); heart (B); and quadriceps (C). Sections were stained with antibodies for CD31 (cyan), LPL (green), and GPIHBP1 (red). DNA was stained with DAPI (blue). Scale bar, 50  $\mu\text{m}$ .

liquid nitrogen. RNA was isolated with TRI reagent (Molecular Research), and quantitative (q)RT-PCR measurements were performed in triplicate on a 7900HT Fast real-time PCR system (Applied Biosystems) (24–26). Gene-expression was calculated with the comparative  $C_T$  method and normalized to cyclophilin A. Primers for *Gpihbp1* were 5'-AGCAGGGACAGAGCACCTCT-3' and 5'-AGACGAGCGTGATGCAGAAG-3' (exons 2/3 and 3, respectively). Primers for *Lpl* were 5'-AGGTGGACATCGGAGA-ACTG-3' and 5'-TCCCTAGCACAGAAGATGACC-3' (exons 8 and 9, respectively).

### Western blot analysis of mouse tissue homogenates

Mice were anesthetized with isoflurane and perfused with PBS. The BAT, heart, lung, and gonadal white adipose tissue (WAT) were harvested. Tissues were homogenized on ice for 12–15 s in 50 mM Tris pH 7.4, 150 mM NaCl, 1 mM EDTA, 1% NP-40, 2.5 mg/ml deoxycholic acid, 0.1% SDS, and Complete EDTA-free protease inhibitor (Roche). Samples were then centrifuged at 15,000  $g$  for 15 min, and the supernatant fluid was collected. Proteins (40  $\mu$ g/lane) were size-fractionated by SDS-PAGE, followed by Western blotting with an IRDye680-conjugated mAb against mouse GPIHBP1 (11A12, 3  $\mu$ g/ml) and a rabbit polyclonal antibody against  $\beta$ -actin (Novus Biologicals; 1:1,000) (followed by an IRDye800-conjugated donkey anti-rabbit IgG from LI-COR). Signals were visualized with an Odyssey infrared scanner (LI-COR).

### Measuring GPIHBP1 on the capillary lumen

Mice were anesthetized with ketamine/xylazine and given an intravenous injection of 30  $\mu$ g IRDye680-conjugated antibody 11A12 in 100  $\mu$ l saline into the inferior vena cava. After 2.5 min, mice were perfused with PBS followed by 3% paraformaldehyde. The BAT, heart, quadriceps, lung, and liver were then harvested and embedded in OCT medium on dry ice. Tissue sections (10  $\mu$ m for BAT, heart, lung, and liver; 20  $\mu$ m for quadriceps) were visualized with an Odyssey scanner (LI-COR). The IRDye680-conjugated 11A12 signal was quantified in each tissue sample and normalized to tissue area (using Image J software).

### Assessing GPIHBP1 monomers and multimers in GPIHBP1-transfected CHO cells

CHO pgsA-745 cells ( $2 \times 10^6$ ) were electroporated with 2  $\mu$ g of a plasmid for S-protein-tagged versions of mouse WT GPIHBP1, GPIHBP1-W108S, or GPIHBP1-C63Y and plated in 24-well plates. After 24 h, cells were treated with phosphatidylinositol-specific phospholipase C (PIPLC; 10 U/ml) in PBS, or PBS alone, for 20 min at 37°C to release GPI-anchored proteins. The PIPLC-released proteins, along with proteins from cell lysates, were analyzed by Western blotting under reducing and nonreducing conditions with antibody 11A12 (3  $\mu$ g/ml) and a goat polyclonal antibody against the S-protein tag (Abcam; 1,000).

### Assessing GPIHBP1 monomers and multimers in the heart

To investigate the presence of GPIHBP1 multimers in vivo, mice were anesthetized with isoflurane and perfused with Tyrode's solution (10 mM HEPES pH 7.4, 136 mM NaCl, 5.4 mM KCl, 0.33 mM  $\text{NaH}_2\text{PO}_4$ , 1 mM  $\text{MgCl}_2$ ) containing 10 mM glucose and 1 mM  $\text{CaCl}_2$ . The heart was then cannulated through the aorta with a blunt 25 gauge needle and perfused with 2 ml of Tyrode's solution. Hearts were then perfused with 800  $\mu$ l of antibody 11A12 (50  $\mu$ g/ml) in Tyrode's solution (or 800  $\mu$ l Tyrode's solution alone) and incubated for 5 min at room temperature. The heart was then perfused with 5 ml of Tyrode's solution. Next, the heart was perfused with 1 ml of Tyrode's solution containing 0.2% Triton X-100. The Triton X-100 perfusate was

then incubated with 25  $\mu$ l of Protein G-agarose beads (ThermoFisher Scientific) for 1 h at 4°C. The beads were washed with Tyrode's solution containing 0.2% Triton X-100 and eluted with SDS sample buffer in the absence of reducing agents (10 min at 90°C). Samples were size-fractionated under nonreducing conditions and processed for Western blotting with an IRDye680-conjugated 11A12 (3  $\mu$ g/ml) and a goat polyclonal antibody against mouse LPL (10  $\mu$ g/ml) (23), followed by an IRDye800-conjugated donkey anti-goat IgG (LI-COR).

### ELISA to measure GPIHBP1 in mouse plasma

ELISA plates were coated with 0.5  $\mu$ g mAb 11A12 (a rat mAb against the carboxyl terminus of mouse GPIHBP1) and incubated overnight at 4°C. The next day, plates were blocked for 4 h at room temperature in Starting block (Pierce). Serial dilutions (1:1, 1:2, 1:4) of frozen mouse plasma samples were added to the wells (40  $\mu$ l/well) and incubated overnight at 4°C. A standard curve with recombinant mouse GPIHBP1 was run in parallel (0–800 pg/well). After washing, the amount of GPIHBP1 captured by antibody 11A12 was tested by adding 50 ng HRP-labeled mAb 2A8 (a rat mAb against the N terminus of mouse GPIHBP1) to each well and incubating for 2 h at 4°C. After washing, the plate was incubated on ice for 15 min with TMB substrate (100  $\mu$ l/well). The reaction was stopped with 2 M sulfuric acid (100  $\mu$ l/well), and the optical density was read at 450 nm.

## RESULTS

Mice harboring a p.C63Y mutation in *Gpihbp1* were generated with CRISPR/Cas9 techniques. DNA sequencing confirmed the presence of the p.C63Y mutation in exon 3 and an absence of any other coding sequence mutations. Mice heterozygous for the mutation (*Gpihbp1*<sup>C63Y/+</sup>) did not have elevated plasma triglyceride levels on a chow diet, whereas homozygous mice (*Gpihbp1*<sup>C63Y/C63Y</sup>) had plasma triglyceride levels >7,000 mg/dl—higher than those in the *Gpihbp1*<sup>-/-</sup> mice within the same colony (Fig. 1).

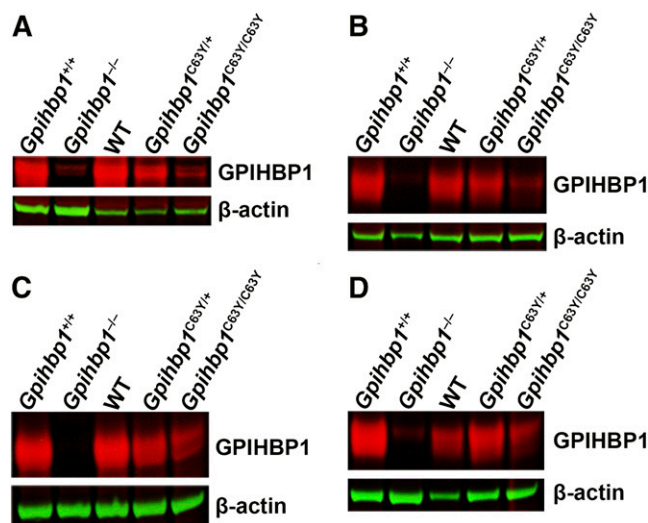


**Fig. 5.** GPIHBP1 protein levels are reduced in tissues of *Gpihbp1*<sup>C63Y/C63Y</sup> mice. Proteins (40  $\mu$ g) from homogenates of heart (A), BAT (B), lung (C), and gonadal WAT (D) were size-fractionated by SDS-PAGE, and Western blots were performed with the GPIHBP1-specific mAb 11A12 (red) and a polyclonal antibody against  $\beta$ -actin (green).

The *Gpihbp1*<sup>C63Y</sup> mutation had little or no effect on *Gpihbp1* expression; the levels of *Gpihbp1* transcripts in BAT and heart were similar in WT, *Gpihbp1*<sup>C63Y/+</sup>, and *Gpihbp1*<sup>C63Y/C63Y</sup> mice (Fig. 2A). *Lpl* transcript levels were also similar (Fig. 2B).

The finding of severe chylomicronemia in *Gpihbp1*<sup>C63Y/C63Y</sup> mice suggested that the mutant GPIHBP1 would not be able to bind LPL. Indeed, mouse GPIHBP1-C63Y had no ability to bind LPL in cell-based LPL–GPIHBP1 binding assays (Fig. 3), and the LPL in BAT was mislocalized within the interstitial spaces—indistinguishable from findings in *Gpihbp1*<sup>-/-</sup> mice (Fig. 4A). The mislocalization of LPL in *Gpihbp1*<sup>C63Y/C63Y</sup> mice was equally apparent in heart and quadriceps (Fig. 4B, C). In these studies, the mutant GPIHBP1 was easily detectable in capillary endothelial cells (Fig. 4A–C).

In some of our immunohistochemistry studies, GPIHBP1 staining was less intense in *Gpihbp1*<sup>C63Y/C63Y</sup> mice than in WT mice, but this finding was inconsistent (Fig. 4). However, Western blots of protein extracts from mouse tissue homogenates unequivocally demonstrated that the amounts of GPIHBP1 protein were lower in *Gpihbp1*<sup>C63Y/C63Y</sup> mice than in WT mice (Fig. 5). Quantification of the Western blot signals revealed that the amounts of GPIHBP1 in the heart, BAT, lung, and gonadal WAT of *Gpihbp1*<sup>C63Y/C63Y</sup>

mice were reduced by 72.4, 77.0, 73.8, and 65.8%, respectively.

The Western blot studies on tissue homogenates obviously could not provide insights into the location of GPIHBP1-C63Y expression (e.g., whether it was on the plasma membrane of endothelial cells or trapped within secretory organelles). For that reason, we used recently validated immunohistochemical methods (21) to determine whether the GPIHBP1 in *Gpihbp1*<sup>C63Y/C63Y</sup> mice was actually present on the luminal surface of capillaries. We injected mice intravenously with an IRDye-labeled mAb against the carboxyl terminus of GPIHBP1 (11A12) and then quantified antibody 11A12 binding to capillaries in tissue sections. The binding of antibody 11A12 to tissues was easily detectable in *Gpihbp1*<sup>C63Y/C63Y</sup> mice—demonstrating that the GPIHBP1-C63Y is present on the luminal surface of endothelial cells; however, the amount of antibody binding was lower in *Gpihbp1*<sup>C63Y/C63Y</sup> mice than in WT mice. Compared with littermate WT mice, amounts of mAb 11A12 binding to heart, BAT, lung, quadriceps, and liver of *Gpihbp1*<sup>C63Y/C63Y</sup> mice were reduced by 79.7, 61.2, 83.3, 70.1, and 39.6% (Fig. 6). Immunohistochemistry studies confirmed that GPIHBP1-C63Y was found on the luminal surface of capillaries (supplemental Fig. S1A, B).

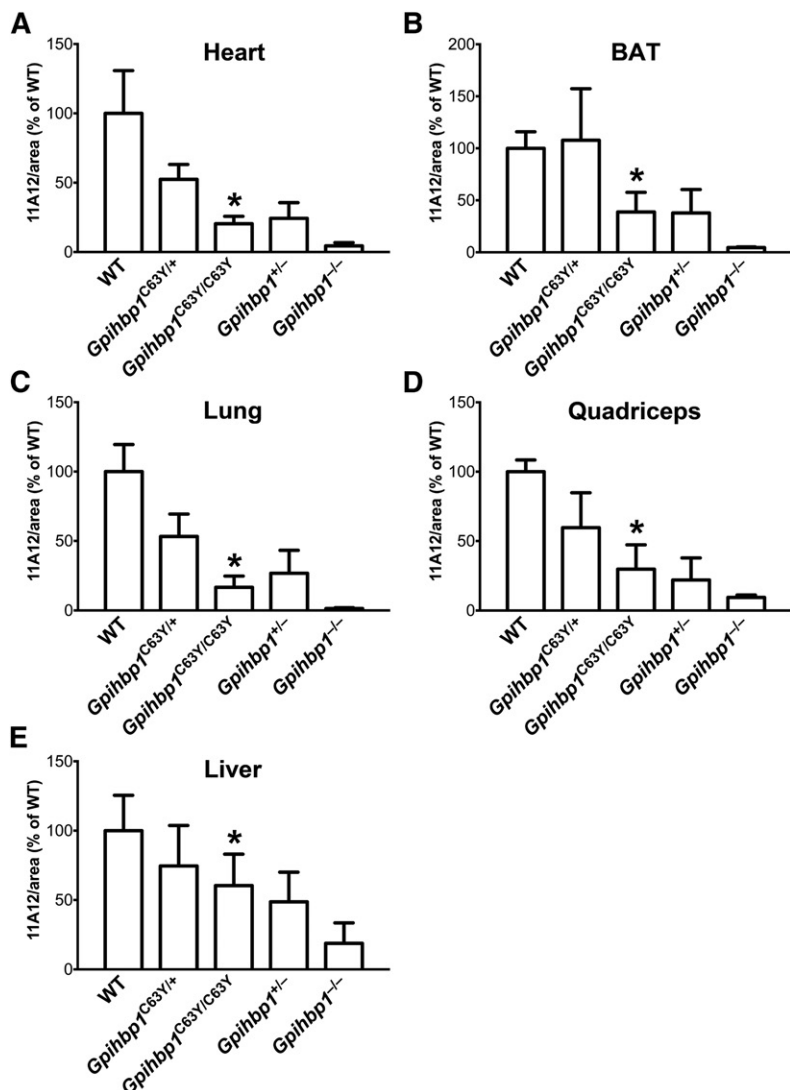


**Fig. 6.** Levels of GPIHBP1 in the capillary lumen are substantially reduced in tissues of *Gpihbp1*<sup>C63Y/C63Y</sup> mice. *Gpihbp1*<sup>C63Y/C63Y</sup> (n = 4), *Gpihbp1*<sup>C63Y/+</sup> (n = 5), and WT (n = 4) mice, along with littermate *Gpihbp1*<sup>-/-</sup> (n = 3) and *Gpihbp1*<sup>+/-</sup> mice (n = 4) (3.5–4 months old), were injected intravenously with IRDye680-labeled 11A12 (30 μg). After 2.5 min, the mice were perfused, and tissues were harvested. Tissue sections from heart (A), BAT (B), lung (C), quadriceps (D), and liver (E) were prepared, and the intensity of the IRDye680 signal was quantified with an Odyssey infrared scanner. The IRDye680 signal (i.e., from labeled mAb 11A12 in the lumen of capillaries) was normalized to tissue area, and the signal in WT mice was set at 100%. GPIHBP1 levels in *Gpihbp1*<sup>C63Y/C63Y</sup> mice were substantially lower than in WT mice (\**P* < 0.0001 for heart, BAT, lung, and quadriceps; \**P* = 0.0055 for liver).

We recently used a pair of human GPIHBP1-specific mAbs to create a sandwich ELISA to measure levels of GPIHBP1 in human plasma (27). Why a GPI-anchored protein such as GPIHBP1 is found in plasma is not known, but we suspect that it is secreted from endothelial cells without a GPI anchor. Here, we took advantage of a pair of mouse-specific GPIHBP1 mAbs (11A12 and 2A8) to create a sandwich ELISA for measuring levels of GPIHBP1 in mouse plasma. GPIHBP1 was easily detectable in the plasma of WT and *Gpihbp1*<sup>C63Y/C63Y</sup> mice, but the levels were somewhat lower in *Gpihbp1*<sup>C63Y/C63Y</sup> mice. As expected, GPIHBP1 was undetectable in plasma samples from *Gpihbp1*<sup>-/-</sup> mice (Fig. 7).

In earlier studies, Beigneux et al. (15) showed, using CHO cell studies, that cysteine mutations in human GPIHBP1 interfere with proper disulfide bond formation and promote the formation of intermolecular disulfide bonds, such that a substantial amount of GPIHBP1 on the surface of cells was in the form of dimers and multimers (15). They also found that substituting Ser for a conserved Trp at residue 109 (Trp-108 in mouse GPIHBP1) resulted in lower-than-normal amounts of GPIHBP1 dimers and multimers. We observed similar findings in mouse GPIHBP1

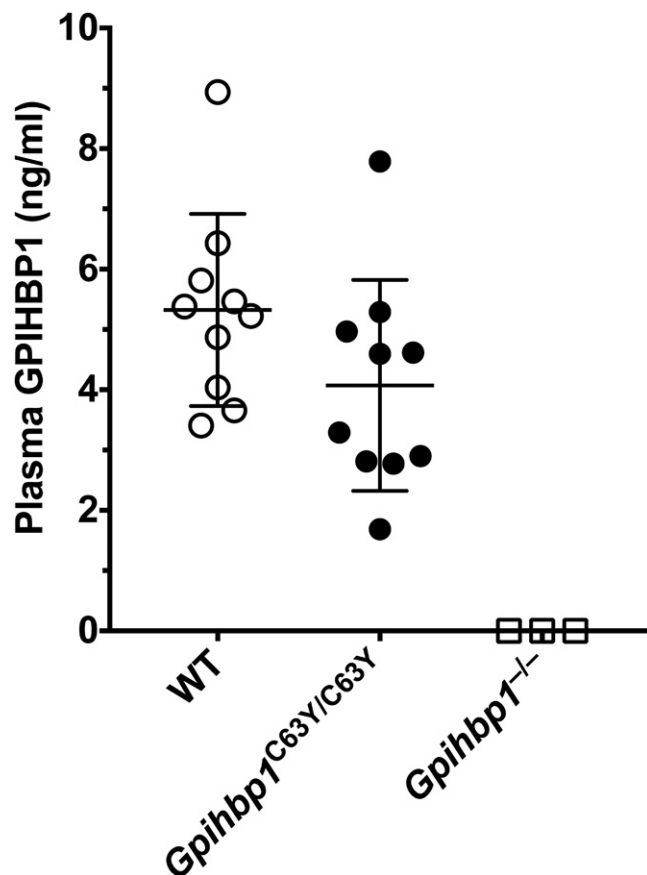


**Fig. 7.** Plasma levels of GPIHBP1 in WT (*Gpihbp1*<sup>+/+</sup>), *Gpihbp1*<sup>C63Y/C63Y</sup>, and *Gpihbp1*<sup>-/-</sup> mice. GPIHBP1 levels in the plasma from 6- to 9-month-old *Gpihbp1*<sup>C63Y/C63Y</sup> mice and WT littermate control mice (n = 10/group) were measured by ELISA. Plasma samples from *Gpihbp1*<sup>-/-</sup> mice (n = 3) were included as controls. GPIHBP1 levels in the plasma were somewhat lower in *Gpihbp1*<sup>C63Y/C63Y</sup> mice than in WT mice, but this difference did not reach statistical significance ( $P = 0.112$ ).

(Fig. 8A). To determine whether GPIHBP1 dimers were present in capillaries of *Gpihbp1*<sup>C63Y/C63Y</sup> mice, we perfused mouse hearts with mAb 11A12, followed by Tyrode's solution. We then released GPIHBP1 from endothelial cells by perfusing the heart with 0.2% Triton X-100. Antibody 11A12 in the perfusate was then immunoprecipitated with Protein G-agarose beads. The immunoprecipitates were size-fractionated by SDS-PAGE under nonreducing conditions, and Western blots were performed with IRDye680-labeled mAb 11A12. Consistent with our findings of reduced amounts of GPIHBP1 in *Gpihbp1*<sup>C63Y/C63Y</sup> tissues (Figs. 5, 6), the amount of GPIHBP1 in the immunoprecipitates from *Gpihbp1*<sup>C63Y/C63Y</sup> hearts were lower than in WT mouse hearts (Fig. 8B). In WT hearts, virtually all of the GPIHBP1 was in the form of monomers (Fig. 8B). In *Gpihbp1*<sup>C63Y/C63Y</sup> mice, the vast majority of the GPIHBP1 was monomeric, but trace amounts of dimers were detected (Fig. 8B). We repeated these studies twice (supplemental Fig. S2). In each experiment, the amount of GPIHBP1 in the immunoprecipitate was reduced in *Gpihbp1*<sup>C63Y/C63Y</sup> hearts. In immunoprecipitates from WT hearts, LPL was detectable along with the GPIHBP1 (reflecting GPIHBP1-bound LPL). Only trace amounts of LPL could be detected in immunoprecipitates from *Gpihbp1*<sup>C63Y/C63Y</sup> hearts and LPL was present regardless of whether the heart had been perfused with mAb 11A12 (supplemental Fig. S2).

## DISCUSSION

Many *GPIHBP1* missense mutations have been identified in patients with chylomicronemia, and most involve conserved cysteines in the Ly6 domain or adjacent residues (6–11, 14). Patients who are homozygous for these missense mutations have reduced amounts of LPL in the plasma (9–11), likely reflecting reduced amounts of LPL in capillaries, but our understanding of how *GPIHBP1* missense mutations cause disease is incomplete. In human subjects, it is not possible to determine whether missense mutations prevent GPIHBP1 from reaching the surface of capillary endothelial cells. Also, no one has determined whether these mutations, which leave GPIHBP1's acidic domain intact, might retain partial function and therefore be associated with less severe disease. To address these issues, we created mice harboring a cysteine-to-tyrosine substitution (p.C63Y) in GPIHBP1. *Gpihbp1*<sup>C63Y/C63Y</sup> mice manifested chylomicronemia, and the LPL in tissues was mislocalized to the interstitial spaces, where it is useless for hydrolyzing triglycerides in the bloodstream. The p.C63Y mutation did not reduce levels of *Gpihbp1* transcripts but nonetheless reduced, by ~70%, amounts of GPIHBP1 protein on capillary endothelial cells. Finding reduced levels of GPIHBP1-C63Y on the plasma membrane of endothelial cells contrasted with virtually normal amounts of mutant GPIHBP1 proteins on the surface of CHO cells (16), but these findings were not altogether surprising, given that mutations of cysteines in CD59 and the LDLR virtually abolished trafficking of those proteins to the cell surface (19, 20, 28, 29). In the case of a cysteine mutation

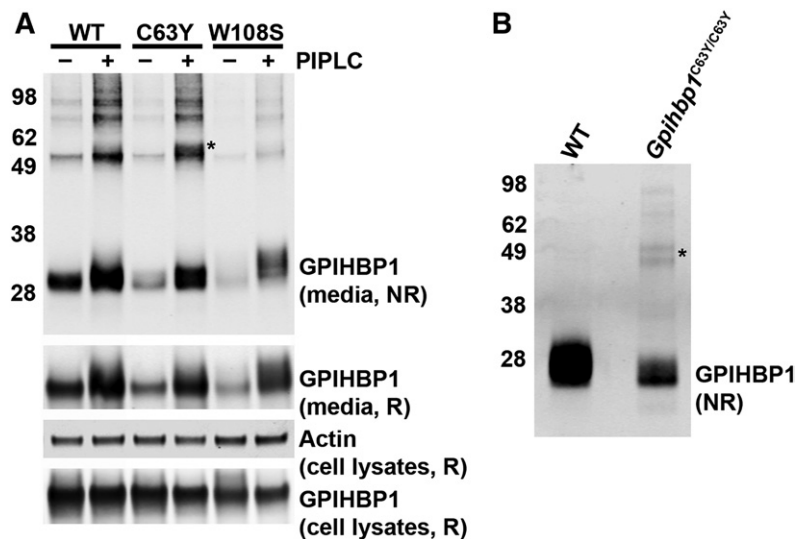


**Fig. 8.** GPIHBP1-C63Y forms large amounts of GPIHBP1 dimers/multimers in CHO cells, but minimal amounts of multimers in heart tissue from *Gpihbp1*<sup>C63Y/C63Y</sup> mice. A: Western blot analysis of S-protein-tagged GPIHBP1 proteins released from the surface of GPIHBP1-transfected CHO pgsA-745 cells with PIPLC. Twenty-four hours after the transfection, the cells were washed and incubated for 20 min at 37°C with PIPLC (10 U/ml). PIPLC-released proteins were size-fractionated by SDS-PAGE under nonreducing (NR) and reducing (R) conditions; cell lysates were examined under reducing conditions. GPIHBP1 was detected with an antibody against the S-protein tag; actin was used as a loading control. GPIHBP1 monomers migrate at ~28 kDa. The GPIHBP1 dimer/multimer-to-monomer ratio was 3.44-fold greater with GPIHBP1-C63Y than with GPIHBP1-W108S, and 1.20-fold higher than with WT GPIHBP1. B: Mouse hearts were isolated and perfused with a mAb against GPIHBP1 (11A12), followed by perfusion with 0.2% Triton X-100. Perfusates were immunoprecipitated with Protein G agarose beads, and eluates from the beads were size-fractionated by SDS-PAGE under nonreducing and reducing conditions. Western blots were performed with an IRDye680-labeled mAb against mouse GPIHBP1 (mAb 11A12). \*Position of GPIHBP1 dimer.

in LDLR, pulse-chase studies in fibroblasts revealed defective trafficking of the mutant LDLR from the ER to the Golgi (29). We suspect that impaired protein trafficking accounts for reduced amounts of GPIHBP1-C63Y on endothelial cells of *Gpihbp1*<sup>C63Y/C63Y</sup> mice. It would obviously be desirable to explore this suspicion with pulse-chase studies in capillary endothelial cells from mice, but these experiments would be next to impossible because *Gpihbp1* expression disappears very rapidly after isolating primary microvascular endothelial cells (30).

While the amount of GPIHBP1 on capillary endothelial cells was reduced in *Gpihbp1*<sup>C63Y/C63Y</sup> mice, we doubt that this finding was responsible for the mislocalization of LPL and the chylomicronemia. Instead, the inability of GPIHBP1-C63Y to bind LPL was almost certainly the primary cause of disease. In CHO cells, substantial amounts of GPIHBP1-C63Y monomers reached the cell surface, but there was little or no LPL binding. Moreover, large amounts of GPIHBP1-C63Y monomers, but little LPL, were released from hearts of *Gpihbp1*<sup>C63Y/C63Y</sup> mice during a short perfusion with 0.2% Triton X-100.


GPIHBP1's Ly6 domain is largely responsible for LPL binding, but the acidic domain contributes to the avidity of LPL-GPIHBP1 interactions (3). GPIHBP1's acidic domain was unaltered by the p.C63Y mutation, but the retention of the acidic domain was not sufficient to permit LPL binding in the CHO cell experiments—or to lessen the severity of the chylomicronemia in mice. The plasma triglyceride levels were clearly not lower in *Gpihbp1*<sup>C63Y/C63Y</sup> mice than in

*Gpihbp1*<sup>-/-</sup> mice, where all GPIHBP1 coding sequences were absent (2).

While developing *Gpihbp1*<sup>C63Y/C63Y</sup> mice, we simultaneously created mice in which all of the acidic residues in GPIHBP1's acidic domain (encoded by exon 2) were replaced with alanine. Our goal was to use these “acidic domain mutant mice” to examine the in vivo functional relevance of the acidic domain. We were delighted that the numerous nucleotide substitutions in exon 2 did not perturb mRNA splicing, but we were disappointed to find that the *Gpihbp1* transcript levels in the mutant mice were reduced by >98%. Not surprisingly, the acidic domain mutant mice manifested severe chylomicronemia. We do not understand why the acidic domain mutations extinguished *Gpihbp1* expression, but it seems possible that exon 2 sequences could serve as a transcriptional enhancer. Others have found evidence for enhancers within protein-coding sequences (31). Alternatively, *Gpihbp1* transcripts lacking exon 2 sequences could be unstable and quickly degraded.

In our studies, we were able to detect GPIHBP1 in mouse plasma with a mAb-based sandwich ELISA. In earlier studies (27), an ELISA detected GPIHBP1 in human plasma. The explanation for the presence of GPIHBP1 in plasma is unknown, but we suspect that small amounts of “soluble GPIHBP1” (GPIHBP1 lacking a GPI anchor) are secreted by capillary endothelial cells. In GPIHBP1-expressing CHO cells, where there is an imbalance between the production of GPIHBP1 and GPI anchors, large amounts of soluble GPIHBP1 are secreted from cells. We suspect that this



same phenomenon occurs, to a lesser degree, in capillary endothelial cells of mice. The amount of GPIHBP1 in the plasma of *Gpihbp1*<sup>C63Y/C63Y</sup> mice was only slightly lower than in WT mice, whereas the amount of GPIHBP1 in tissues of *Gpihbp1*<sup>C63Y/C63Y</sup> mice was reduced by ~70%. We do not fully understand this discrepancy, but it is possible that soluble GPIHBP1-C63Y is more capable of avoiding the quality-control surveillance mechanisms in the ER. In support of this idea, eliminating the N-linked glycosylation site in a full-length GPIHBP1 markedly reduced GPIHBP1 trafficking to the surface of CHO cells (18), whereas the glycosylation site mutation had minimal effects on the secretion of soluble GPIHBP1 (a GPIHBP1 that was truncated before the GPI-anchoring site) (18). 

## REFERENCES

- Davies, B. S., A. P. Beigneux, R. H. Barnes II, Y. Tu, P. Gin, M. M. Weinstein, C. Nobumori, R. Nyren, I. Goldberg, G. Olivecrona, et al. 2010. GPIHBP1 is responsible for the entry of lipoprotein lipase into capillaries. *Cell Metab.* **12**: 42–52.
- Beigneux, A. P., B. Davies, P. Gin, M. M. Weinstein, E. Farber, X. Qiao, P. Peale, S. Bunting, R. L. Walzem, J. S. Wong, et al. 2007. Glycosylphosphatidylinositol-anchored high density lipoprotein-binding protein 1 plays a critical role in the lipolytic processing of chylomicrons. *Cell Metab.* **5**: 279–291.
- Mysling, S., K. K. Kristensen, M. Larsson, A. P. Beigneux, H. Gardsvoll, L. G. Fong, A. Bensadoun, T. J. Jorgensen, S. G. Young, and M. Ploug. 2016. The acidic domain of the endothelial membrane protein GPIHBP1 stabilizes lipoprotein lipase activity by preventing unfolding of its catalytic domain. *eLife*. **5**: e12095.
- Fry, B. G., W. Wuster, R. M. Kini, V. Brusica, A. Khan, D. Venkataraman, and A. P. Rooney. 2003. Molecular evolution and phylogeny of elapid snake venom three-finger toxins. *J. Mol. Evol.* **57**: 110–129.
- Gin, P., L. Yin, B. S. J. Davies, M. M. Weinstein, R. O. Ryan, A. Bensadoun, L. G. Fong, S. G. Young, and A. P. Beigneux. 2008. The acidic domain of GPIHBP1 is important for the binding of lipoprotein lipase and chylomicrons. *J. Biol. Chem.* **283**: 29554–29562.
- Beigneux, A. P., R. Franssen, A. Bensadoun, P. Gin, K. Melford, J. Peter, R. L. Walzem, M. M. Weinstein, B. S. Davies, J. A. Kuivenhoven, et al. 2009. Chylomicronemia with a mutant GPIHBP1 (Q115P) that cannot bind lipoprotein lipase. *Arterioscler. Thromb. Vasc. Biol.* **29**: 956–962.
- Charrière, S., N. Peretti, S. Bernard, M. Di Filippo, A. Sassolas, M. Merlin, M. Delay, C. Debar, E. Lefai, A. Lachaux, et al. 2011. GPIHBP1 C89F neomutation and hydrophobic C-terminal domain G175R mutation in two pedigrees with severe hyperchylomicronemia. *J. Clin. Endocrinol. Metab.* **96**: E1675–E1679.
- Coca-Prieto, I., O. Kroupa, P. Gonzalez-Santos, J. Magne, G. Olivecrona, E. Ehrenborg, and P. Valdivielso. 2011. Childhood-onset chylomicronemia with reduced plasma lipoprotein lipase activity and mass: identification of a novel GPIHBP1 mutation. *J. Intern. Med.* **270**: 224–228.
- Franssen, R., S. G. Young, F. Peelman, J. Hertecant, J. A. Sierts, A. W. M. Schimmel, A. Bensadoun, J. J. P. Kastelein, L. G. Fong, G. M. Dallinga-Thie, et al. 2010. Chylomicronemia with low postheparin lipoprotein lipase levels in the setting of GPIHBP1 defects. *Circ Cardiovasc Genet.* **3**: 169–178.
- Olivecrona, G., E. Ehrenborg, H. Semb, E. Makoveichuk, A. Lindberg, M. R. Hayden, P. Gin, B. S. J. Davies, M. M. Weinstein, L. G. Fong, et al. 2010. Mutation of conserved cysteines in the Ly6 domain of GPIHBP1 in familial chylomicronemia. *J. Lipid Res.* **51**: 1535–1545.
- Plengpanich, W., S. G. Young, W. Khovidhunkit, A. Bensadoun, H. Karnman, M. Ploug, H. Gardsvoll, C. S. Leung, O. Adeyo, M. Larsson, et al. 2014. Multimerization of GPIHBP1 and familial chylomicronemia from a serine-to-cysteine substitution in GPIHBP1's Ly6 domain. *J. Biol. Chem.* **289**: 19491–19499.
- Rios, J. J., S. Shastry, J. Jasso, N. Hauser, A. Garg, A. Bensadoun, J. C. Cohen, and H. H. Hobbs. 2012. Deletion of GPIHBP1 causing severe chylomicronemia. *J. Inher. Metab. Dis.* **35**: 531–540.
- Patni, N., J. Brothers, C. Xing, and A. Garg. 2016. Type 1 hyperlipoproteinemia in a child with large homozygous deletion encompassing GPIHBP1. *J. Clin. Lipidol.* **10**: 1035–1039.e2.
- Surendran, R. P., M. E. Visser, S. Heemelaar, J. Wang, J. Peter, J. C. Defesche, J. A. Kuivenhoven, M. Hosseini, M. Peterfy, J. J. Kastelein, et al. 2012. Mutations in LPL, APOC2, APOA5, GPIHBP1 and LMF1 in patients with severe hypertriglyceridaemia. *J. Intern. Med.* **272**: 185–196.
- Beigneux, A. P., L. G. Fong, A. Bensadoun, B. S. Davies, M. Oberer, H. Gardsvoll, M. Ploug, and S. G. Young. 2015. GPIHBP1 missense mutations often cause multimerization of GPIHBP1 and thereby prevent lipoprotein lipase binding. *Circ. Res.* **116**: 624–632.
- Beigneux, A. P., P. Gin, B. S. J. Davies, M. M. Weinstein, A. Bensadoun, L. G. Fong, and S. G. Young. 2009. Highly conserved cysteines within the Ly6 domain of GPIHBP1 are crucial for the binding of lipoprotein lipase. *J. Biol. Chem.* **284**: 30240–30247.
- Beigneux, A. P., B. S. J. Davies, S. Tat, J. Chen, P. Gin, C. V. Voss, M. M. Weinstein, A. Bensadoun, C. R. Pullinger, L. G. Fong, et al. 2011. Assessing the role of the glycosylphosphatidylinositol-anchored high density lipoprotein-binding protein 1 (GPIHBP1) three-finger domain in binding lipoprotein lipase. *J. Biol. Chem.* **286**: 19735–19743.
- Beigneux, A. P., P. Gin, B. S. Davies, M. M. Weinstein, A. Bensadoun, R. O. Ryan, L. G. Fong, and S. G. Young. 2008. Glycosylation of Asn-76 in mouse GPIHBP1 is critical for its appearance on the cell surface and the binding of chylomicrons and lipoprotein lipase. *J. Lipid Res.* **49**: 1312–1321.
- Goldstein, J. L., M. S. Brown, R. G. W. Anderson, D. W. Russell, and W. J. Schneider. 1985. Receptor-mediated endocytosis: concepts emerging from the LDL receptor system. *Annu. Rev. Cell Biol.* **1**: 1–39.
- Petrankska, J., J. Zhao, J. Norris, N. B. Tweedy, R. E. Ware, P. J. Sims, and W. F. Rosse. 1996. Structure-function relationships of the complement regulatory protein, CD59. *Blood Cells Mol. Dis.* **22**: 281–296.
- Goulbourne, C. N., P. Gin, A. Tatar, C. Nobumori, A. Hoenger, H. Jiang, C. R. Grovenor, O. Adeyo, J. D. Esko, I. J. Goldberg, et al. 2014. The GPIHBP1-LPL complex is responsible for the margination of triglyceride-rich lipoproteins in capillaries. *Cell Metab.* **19**: 849–860.
- Ben-Zeev, O., H. Z. Mao, and M. H. Doolittle. 2002. Maturation of lipoprotein lipase in the endoplasmic reticulum. Concurrent formation of functional dimers and inactive aggregates. *J. Biol. Chem.* **277**: 10727–10738.
- Page, S., A. Judson, K. Melford, and A. Bensadoun. 2006. Interaction of lipoprotein lipase and receptor-associated protein. *J. Biol. Chem.* **281**: 13931–13938.
- Weinstein, M. M., C. N. Goulbourne, B. S. Davies, Y. Tu, R. H. Barnes II, S. M. Watkins, R. Davis, K. Reue, P. Tontonoz, A. P. Beigneux, et al. 2012. Reciprocal metabolic perturbations in the adipose tissue and liver of GPIHBP1-deficient mice. *Arterioscler. Thromb. Vasc. Biol.* **32**: 230–235.
- Jung, H. J., C. Nobumori, C. N. Goulbourne, Y. Tu, J. M. Lee, A. Tatar, D. Wu, Y. Yoshinaga, P. J. de Jong, C. Coffinier, et al. 2013. Farnesylation of lamin B1 is important for retention of nuclear chromatin during neuronal migration. *Proc. Natl. Acad. Sci. USA.* **110**: E1923–E1932.
- Yang, S. H., S. Y. Chang, L. Yin, Y. Tu, Y. Hu, Y. Yoshinaga, P. J. de Jong, L. G. Fong, and S. G. Young. 2011. An absence of both lamin B1 and lamin B2 in keratinocytes has no effect on cell proliferation or the development of skin and hair. *Hum. Mol. Genet.* **20**: 3537–3544.
- Hu, X., M. Sleeman, K. Miyashita, M. F. Linton, C. M. Allan, C. He, M. Larsson, N. P. Sandoval, R. S. Jung, A. Mapar, et al. 2017. Monoclonal antibodies that bind to the Ly6 domain of GPIHBP1 abolish the binding of LPL. *J. Lipid Res.* **58**: 208–215.
- Leitersdorf, E., E. J. Tobin, J. Davignon, and H. H. Hobbs. 1990. Common low-density lipoprotein receptor mutations in the French Canadian population. *J. Clin. Invest.* **85**: 1014–1023.
- Esser, V., and D. W. Russell. 1988. Transport-deficient mutations in the low density lipoprotein receptor. Alterations in the cysteine-rich and cysteine-poor regions of the protein block intracellular transport. *J. Biol. Chem.* **263**: 13276–13281.
- Davies, B. S. J., H. Waki, A. P. Beigneux, E. Farber, M. M. Weinstein, D. C. Wilpitz, L.-J. Tai, R. M. Evans, L. G. Fong, P. Tontonoz, et al. 2008. The expression of GPIHBP1, an endothelial cell binding site for lipoprotein lipase and chylomicrons, is induced by peroxisome proliferator-activated receptor-gamma. *Mol. Endocrinol.* **22**: 2496–2504.
- Ritter, D. I., Z. Dong, S. Guo, and J. H. Chuang. 2012. Transcriptional enhancers in protein-coding exons of vertebrate developmental genes. *PLoS One.* **7**: e35202.